World Academy of Science, Engineering and Technology
International Journal of Mechanical and Mechatronics Engineering
Vol:3, No:12, 2009

Capsule-substrate Adhesion in the Presence of Osmosis by the Immersed Interface Method

P.G. Jayathilake, B.C. Khoo, Zhijun Tan

Abstract**—**A two-dimensional thin-walled capsule of a flexible semi-permeable membrane is adhered onto a rigid planar substrate under adhesive forces (derived from a potential function) in the presence of osmosis across the membrane. The capsule is immersed in a hypotonic and diluted binary solution of a non-electrolyte solute. The Stokes flow problem is solved by the immersed interface method (IIM) with equal viscosities for the enclosed and surrounding fluid of the capsule. The numerical results obtained are verified against two simplified theoretical solutions and the agreements are good. The osmotic inflation of the adhered capsule is studied as a function of the solute concentration field, hydraulic conductivity, and the initial capsule shape. Our findings indicate that the contact length shrinks in dimension as capsule inflates in the hypotonic medium, and the equilibrium contact length does not depend on the hydraulic conductivity of the membrane and the initial shape of the capsule.

Keywords**—**Capsule-substrate adhesion, Fluid mechanics, Immersed interface method, Osmosis, Mass transfer.

I. INTRODUCTION

CAPSULES of thin elastic membranes enclosing incompressible viscous liquid are commonly employed as models for study in many biological and industrial systems. The flow induced-deformation of capsules has been studied by researchers in past two decades to investigate the effects of membrane elasticity, membrane rigidity, membrane and fluid viscosities and inertia of the flow field, etc on capsule deformation. In extension to study the dynamics of capsule adhesion onto a planar or curved substrate is deemed important as far as biological and biophysical applications are concerned. For example, adhesion of leukocytes (while blood cells) to vascular endothelium is a key process in inflammatory response ([1]). Previous numerical studies on capsule-substrate adhesion have investigated effects of material, geometrical and flow properties on capsule adhesion and deformation under shear flows (see [2-5]).

If capsule membrane is permeable, the capsule-substrate adhesion is also controlled by the surrounding environment ([6]). Several extensive experimental works on capsule adhesion in the presence of osmosis can be seen in the literature such as [7] which has shown empirically the effect of osmotic pressure on adhesion between a vesicle and a glass slide. An experimental method combined with a theoretical model to calculate unknown membrane and adhesion properties of a capsule-substrate adhesion system with osmosis has been provided in [8]. Among other theoretical works, some studies on coupled bending-shearing on liposome deformation under different osmotic pressures have been studied in [9], [10], and the results have shown that degree of liposome deformation is larger when the bending is dominant and the adhesion contact area increases when liposome volume decreases. A good agreement between their experimental and theoretical results can be seen in [9]. A simple elastic model based on energy balance to compute the final equilibrium shape of a spherical capsule adhered to a planar substrate in the presence of osmosis has been provided in [6], [11], and the relationships between osmotic inflation, contact area and contact angle have been studied. The possibility of determining the adhesion strength between a liquid-filled capsule and a planer substrate via the aforementioned elastic model has been demonstrated later on ([12], [13]). All these theoretical models have been used to calculate the final equilibrium shape of the adhered capsule for given physical parameters. To the best of authors' knowledge there are hardly any (numerical) studies on capsule adhesion in the presence of osmosis.

In the present work, a new numerical model based on the immersed interface method (IIM) to simulate capsule adhesion onto a planar substrate in the presence of osmosis is presented. In the literature, there are numerous works on developing efficient computational techniques for simulating problems involving fluid flow with immersed impermeable deformable boundaries or membranes. Perhaps one of the most important developments in the past decades or so is the immersed boundary method (IB Method or IBM) by Peskin [14] with basically first order accuracy. The IB method is a very robust numerical method for solving the full

P. G. Jayathilake is with the Department of Mechanical Engineering, National University of Singapore, Kent Ridge Crescent, Singapore 119260, Singapore (phone: +65 96613940; fax: +65 67791459; email: g0501295@nus.edu.sg).

B. C. Khoo is with the Department of Mechanical Engineering, National University of Singapore, Kent Ridge Crescent, Singapore 119260, Singapore, and Singapore-MIT Alliance, 4 Engineering Drive 3, National University of Singapore, Singapore 117576, Singapore (email: mpekbc@nus.edu.sg).

Zhijun Tan is with Singapore-MIT Alliance, 4 Engineering Drive 3, National University of Singapore, Singapore 117576, Singapore (email:smatz@nus.edu.sg).

incompressible Navier-Stokes equations with immersed impermeable moving boundaries. The IB method has been used by subsequent researchers to simulate transient rolling adhesion and deformation of cells in the absence of osmosis ([5], [15], [16]). Partially motivated from the IB method, the immersed interface method (IIM) was developed by LeVeque and Li [17] with second order accuracy and applied for two-dimensional models. The IIM has seen more advancement by many subsequent researchers for problems involving immersed impermeable deformable boundaries ([18-26]). The key idea of the method is to find coefficients of a new finite difference scheme at irregular grid points by using the information of the field variable and its normal derivative near the boundary. As the IIM is more accurate for moving immersed impermeable boundary problems, it is naturally extended to problems involving deformable and permeable boundary problems. As reported in [27], the IIM was also used to model the mass transfer across a semi-permeable deformable capsule suspended in an aqueous solution under Stokes flow for a limited case. In that work, while the Stokes equations has been solved using the IIM approach mentioned in [22], a new time-split method has been employed to solve for the mass transport equation near the capsule membrane.

In this paper, a two-dimensional numerical model based on the IIM is presented to simulate capsule-substrate adhesion in the presence of osmosis under a variety of conditions for a careful and systematic study of the capsule-substrate adhesion. The rest of this paper is organized as follows. In Section II, the governing equations and numerical calculation procedure based on the IIM for a general capsule-substrate adhesion problem with osmosis (see Fig. 1) are described. Section III gives the results and discussions for various cases, and Section IV provides the conclusions for the present study.

II. MODEL FORMULATION

A flat semi-permeable closed thin membrane Γ is allowed to move from its initial configuration due to unbalanced forces under the Stokes flow condition. These unbalanced forces may arise from elastic forces or adhesive forces or osmotic pressure difference across the membrane. The membrane separates the whole fluid domain Ω into two domains as Ω^- and Ω^+, where Ω^- is the region enclosed by the membrane whereas Ω^+ is the region outside of the membrane as illustrated in Fig. 1 (the combination of Γ and Ω^- is called a capsule). Both domains are filled with a non-electrolyte diluted binary solution of different solute concentrations. The membrane and fluid properties are assumed to be constant.
The governing equations are thus given as follows:

$$p_x(x,y,t) = \mu(u_{xx}(x,y,t) + u_{yy}(x,y,t)) + F_1(x,y,t), \quad (1)$$

$$p_y(x,y,t) = \mu(v_{xx}(x,y,t) + v_{yy}(x,y,t)) + F_2(x,y,t), \quad (2)$$

$$u_x(x,y,t) + v_y(x,y,t) = 0, \quad (3)$$

$$c_t + uc_x + vc_y = D(c_{xx} + c_{yy}), \quad (4)$$

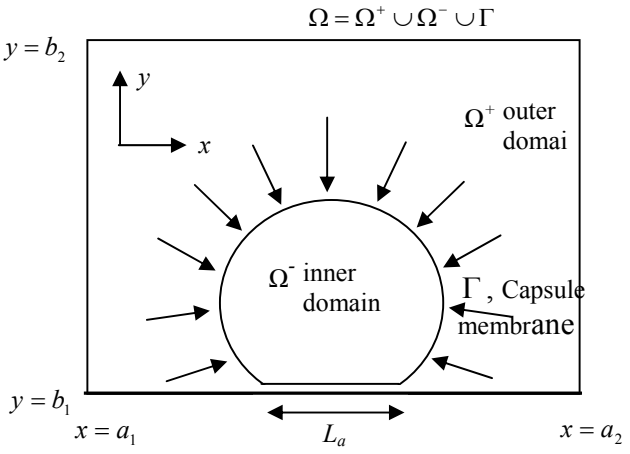

Fig. 1 Capsule-substrate adhesion in the presence of osmosis.

where (x, y, t) is the spatial position and time, respectively, p is the fluid pressure (or mechanical pressure), (u, v) is the fluid velocity in the x and y directions, respectively, c is the solute concentration, μ the dynamic viscosity of fluid, a constant throughout Ω, D is the solute diffusivity, a constant throughout Ω, and F_1, F_2 is the singular force that arises from the interface in the x and y directions, respectively. The subscript (x) represents the derivative taken with respect to (x) and so on. The singular forces F_1 and F_2 can be calculated as

$$F_l(\vec{x},t) = \int_\Gamma f_l(s,t)\delta_D(\vec{x} - \vec{X}(s,t))\,ds, \quad (5)$$

for l = 1, 2, which represents the x and y directions, respectively. $\vec{x}(x,y)$ is the spatial position, $\vec{X}(s,t)$ is the membrane configuration Γ, s is the length measured along the membrane, f_l is the force strength in either x or y direction, and δ_D is the two-dimensional Dirac delta function. The resultant force strength $\vec{f}$ is given by

$$\vec{f}(s,t) = \frac{\partial}{\partial s}\left(T_e(s,t)\vec{\tau}(s,t) + T_b(s,t)\vec{n}(s,t)\right) - \frac{\partial W}{\partial y}\hat{y}, \quad (6)$$

where T_e, T_b and W are the elastic tension, shear tension due to bending and adhesion potential between the capsule and substrate, respectively. These are given by

$T_e = E_e(\varepsilon^{1.5} - \varepsilon^{-1.5})$, $T_b = \frac{\partial}{\partial s}\left[E_b(\kappa - \kappa_R\right]$, and

$W = W_{ad}\left[\left(\frac{d_m}{y}\right)^4 - 2\left(\frac{d_m}{y}\right)^2\right]$. Here, $\vec{\tau}$, $\vec{n}$ and $\hat{y}$ are unit vectors defined at any point on the membrane and their respective directions are the anticlockwise tangential, the outward normal and the y direction. The physical parameters E_e, E_b and W_{ad} are the membrane shear modulus, bending modulus and adhesion strength, respectively. κ is the

membrane curvature at any point while κ_R is the reference curvature. ε is the stretch ratio of the membrane and the optimal distance (or zero force distance) between the membrane and substrate is d_m.

For the semi-permeable membrane, some solvent could pass across the membrane, and hence the membrane velocity $\vec{U} = (U, V)$ to be calculated is given below as ([27]):

$$U(\vec{X}(s,t),t) = u(\vec{X}(s,t),t) - J_v(s,t).\cos(\theta), \quad (7)$$

$$V(\vec{X}(s,t),t) = v(\vec{X}(s,t),t) - J_v(s,t).\sin(\theta), \quad (8)$$

where θ is the angle between the normal line to the membrane and the x-axis at any point on the membrane and J_v is the solvent volume flux across the membrane. The solvent volume flux is calculated using the Kedem-Katchalsky relation for binary diluted solutions ([28]). This equation has been obtained using irreversible thermodynamics theory for coupled-flows of solutes and solvent as follows:

$$J_v = -L_P([p] - RT_{abs}[c]), \quad (9)$$

where J_v is the solvent volume flux (m^3/m^2 s, or m/s), R is the universal gas constant (J/mol.K), T_{abs} is the absolute temperature (K), $[p]$ is the mechanical pressure jump (or difference) across the membrane (or interface) (N/m^2), $[c]$ is the solute concentration jump across the membrane (mol/m^3), L_p is the hydraulic conductivity of the membrane ($m^2.s/kg$). The jump of a variable ψ is defined at any point on the membrane and is given by

$$[\psi(\vec{X})] = \psi(\vec{X}^+ + \zeta.\vec{n}) - \psi(\vec{X}^- - \zeta.\vec{n}) \text{ as } \zeta \to 0^+.$$

Boundary conditions

The Dirichlet boundary condition for the velocity (u, v) and Neumann boundary condition for both pressure (p) and solute concentration (c) are assumed applicable along the boundary of the computational domain Ω. The solute molar flux at either side of the membrane is equal to zero since the membrane is semi-permeable, and it is given by

$$[J_v.c - D.c_n]_{\Gamma^-} = [J_v.c - D.c_n]_{\Gamma^+} = 0, \quad (10)$$

where c_n is the derivative of c with respect to the normal outward direction ($\vec{n}$) to the membrane.

All the equations are non-dimensionalized via the suitable reference values for different variables. The reference values are defined for length $\bar{r}$ (≡ unstretched capsule radius), velocity $\bar{V}$ (≡ $\bar{L}_p RT_{abs}\Delta c_0$), pressure $\bar{p}$ (≡ $\mu\bar{V}/\bar{r}$), time $\bar{t}$ (≡ $\bar{r}/\bar{V}$), membrane tension $\bar{T}$ (≡ E_e) and solute concentration $\bar{c}$ (≡ $[c_0]/\ln(c_0^+/c_0^-)$). Here Δc_0 is the initial solute concentration difference across the membrane (i.e., $\Delta c_0 = |c_0^+ - c_0^-|$) and $c_0^{\pm}$ is the initial constant solute concentration at either side of the membrane. $\bar{L}_p$ is the reference value of the hydraulic conductivity.

All the non-dimensional variables are denoted with an asterisk (*) mark. Then the governing Eqs. (1)-(4) and (9) can be written in non-dimensional form and given below as

$$p^*_{x^*} = (u^*_{x^*x^*} + u^*_{y^*y^*}) + F_1^*, \quad (11)$$

$$p^*_{y^*} = (v^*_{x^*x^*} + v^*_{y^*y^*}) + F_2^*, \quad (12)$$

$$u^*_{x^*} + v^*_{y^*} = 0, \quad (13)$$

$$c^*_{t^*} + u^* c^*_{x^*} + v^* c^*_{y^*} = \frac{1}{Pe}(c^*_{x^*x^*} + c^*_{y^*y^*}), \quad (14)$$

$$J_v^* = -\frac{L_p}{\bar{L}_p}\left(f_N^*.\delta - \frac{[c^*]}{\ln\gamma}\right), \quad (15)$$

where f_N^* is the force strength in the $\vec{n}$ direction. $\delta = \frac{E_e/\bar{r}}{RT_{abs}\Delta c_0}$, $\gamma = \frac{c_0^-}{c_0^+}$, $Pe = \frac{\bar{V}\bar{r}}{D}$, and they represent, respectively, the ratio between the elastic and osmotic pressure differences across the membrane, the initial solute concentration ratio between the inner and outer domains, and the ratio between the convective and diffusive mass transport in fluid (Peclet number).

Hereafter, the asterisk (*) mark is dropped from the non-dimensional variables for simplicity.

A. Numerical methods

The whole computational domain $\Omega = [a_1, a_2] \times [b_1, b_2]$ is discretized into M+1 and N+1 grid points in the x and y directions, respectively. The capsule membrane Γ is represented by N_b points which are called control points. The spatial grid size, $h = (a_2 - a_1)/M = (b_2 - b_1)/N$.

For the given membrane configuration (X^m, Y^m), primitive variables (p^m, u^m, v^m) and solute concentration (c^m) at $t = t^m$, the variables p^{m+1}, u^{m+1}, v^{m+1}, c^{m+1} and (X^{m+1}, Y^{m+1}) are to be calculated for $t = t^{m+1}$. The membrane configuration is updated explicitly as

$$X^{m+1} = X^m + \Delta t.U^m,$$

$$Y^{m+1} = Y^m + \Delta t.V^m,$$

where Δt is the non-dimensional time step.

Following [29], the governing equations of motion Eqs. (11)-(13) are decoupled into three equations as $\nabla^2 p = \nabla\vec{F}$, $\nabla^2 u = p_x$ and $\nabla^2 v = p_y$. These three Poisson equations are discretized according to the IIM and solved using the FISHPACK fast solvers ([22]).

Once the primitive variables p^{m+1}, u^{m+1}, v^{m+1} and the membrane position (X^{m+1}, Y^{m+1}) are calculated, the solute concentration field at t^{m+1} is updated according to Eq. (14). This equation is solved fairly similar to the approach in [27] using the IIM .The diffusive term is discretized implicitly

while the convective term is treated explicitly to avoid restriction on Δt, hence giving rise to

$$\frac{c_{i,j}^{m+1}-c_{i,j}^{m}}{\Delta t}+Q_{i,j}-\frac{1}{Pe}\left\{\nabla^2 c_{i,j}^{m+1}+C_{i,j}(\nabla^2 c\ )\right\}= -u_{i,j}^{m}\left\{c_{x,i,j}^{m}+C_{i,j}(c_x)\right\}-v_{i,j}^{m}\left\{c_{y,i,j}^{m}+C_{i,j}(c_y^{m}\right\}, \tag{16}$$

where $C_{i,j}(\nabla^2 c)$ is the spatial correction term of $\nabla^2 c$ which is added only at irregular grid point (i, j) and so on. $Q_{i,j}$ is the temporal correction term and it is non-zero if the grid point (i, j) is crossed by the membrane at a time between t^m and t^{m+1}. The derivations using Taylor series expansions and detailed discussions about these correction terms can be found in the literature and not repeated here ([20], [29], [30]).

B. Jump conditions for the IIM

When using the IIM to solve the governing equations in a domain with an immersed membrane, the jumps of the field variable and its normal derivative across the membrane are needed to calculate previously mentioned correction terms near the membrane (i.e., $C_{i,j}$ and $Q_{i,j}$) . Thus jumps of pressure, velocity, concentration and jumps of their normal derivatives are required. These jump conditions for variables p, u and v are given as

$$\begin{aligned}
&[p]=\beta f_N,\\
&[p_n]=\beta\frac{\partial}{\partial s}f_T,\\
&[u]=[v]=0,\\
&[u_n]=\beta f_T\sin\theta,\\
&[v_n]=-\beta f_T\cos\theta,
\end{aligned} \tag{17}$$

where $\beta = E_e / \mu\overline{V}$, f_N and f_T are the non-dimensional form of the normal and tangential components of the force strength $\vec{f}$. These jump conditions are derived using the equations of motion Eqs. (11)-(13) as seen in [22].

Since the solute concentration jump conditions ([c], [c_n]) are not available explicitly, those jump conditions are calculated numerically with use of the Kedem-Katchalsky relation (Eq. (15)) (see [31] for detailed implementation as only brief discussion is provided here). In this approach, at each control point, four points are defined along the normal line to the membrane as $\overrightarrow{X}^m \pm qh$, where q = 1, 2, and these are named as (k, 1), (k, 2), (k, 3) and (k, 4) at the k^{th} control point as illustrated in Fig. 2. Then, nearby three grid point concentration values are interpolated using the one-sided least squares method to calculate the solute concentration value at each of above defined points. These interpolated concentration values at respective points are denoted by $c_{k,1}, c_{k,2}, c_{k,3}$ and $c_{k,4}$. The boundary concentration values at the k^{th} control point are c_k^- and c_k^+ in Γ^- and Γ^+ sides, respectively.

With discretizing the non-dimensional form of Eq. (10) along the normal direction ($\vec{n}$) in either side of the membrane ($\Gamma^{\pm}$), the boundary solute concentration values at the immediate sides of the membrane are calculated for $t = t^{m+1}$ as

$$\begin{aligned}
c_k^{-,m+1}&=\frac{\left(4c_{k,1}^{m+1}-c_{k,2}^{m+1}\right)}{3-2hPeJ_{v,k}^{m}},\\
c_k^{+,m+1}&=\frac{\left(4c_{k,3}^{m+1}-c_{k,4}^{m+1}\right)}{3+2hPeJ_{v,k}^{m}}.
\end{aligned} \tag{18}$$

Hence, the solute concentration jumps across the membrane are calculated as

$$[c_{\ k}\ ]^{m+1}=c_k^{+,m+1}-c_k^{-,m+1},\quad k=1,2,\ldots,N_b.$$

By writing the non-dimensional form of Eq. (10) at immediate sides of the membrane, it is obtained that

$$[c_{n,k}]^{m+1}=J_v^{m+1}Pe\left(c_k^{+,m+1}-c_k^{-,m+1}\right),\quad k=1,2,\ldots,N_b.$$

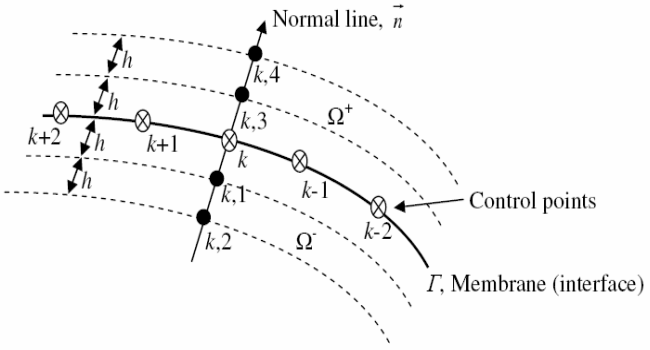

Fig. 2 Sketch for the calculation of the solute concentration values along a normal line to the membrane.

III. NUMERICAL RESULTS AND DISCUSIONS

Two set of numerical simulations are performed; one for capsule adhesion in the absence of osmosis (L_p = 0) and another for capsule adhesion in the presence of osmosis (L_p > 0). In both cases, validations against theoretical results are given for the numerical results whenever possible.

The values of physical parameters are chosen so that these are in the range for typical biological systems. The dimensions of the computational domain are a_1 = b_1 = -10 μm and a_2 = b_2 = 10 μm. The unstretched initial circular capsule has a radius of 4 μm. The planer substrate coincides with y = b_1 line (see Fig. 1). The physical parameters of the membrane and fluid are chosen as E_e = 43 μN/m, E_b = 1.8x10^{-13} μJ, μ = 4x10^{-3} N.s/m^2, T_{abs} = 300 K and D = 1.5x10^{-9} m^2/s. The universal gas

constant is R = 8.314 J/mol.K. The adhesion strength is in the range of W_{ad} = 4.11-4.11x10^{-2} μJ/m^2 and it falls in the biological range ([32]). All calculations are carried out with $M = N = N_b$ = 80. (It should be noted that when values of variables are given along with their respective units, those values are in the dimensional form.)

For the boundary conditions, zero velocity and zero solute flux are imposed along the boundary of the computational domain Ω (i.e., $u = v = 0$ and $\left(\frac{\partial c}{\partial x}\right)_{x=a_1,a_2} = \left(\frac{\partial c}{\partial y}\right)_{y=b_1,b_2} = 0$). The Neumann boundary condition for the pressure is calculated based on the augmented approach in [29]. In this approach, $\left(\frac{\partial p}{\partial x}\right)_{x=a_1,a_2}$ and $\left(\frac{\partial p}{\partial y}\right)_{y=b_1,b_2}$ are represented by unknown variables p_{n1}, p_{n2}, p_{n3}…at grid points along the boundary of Ω and they are calculated using Eqs. (11)-(13).

A. Adhesion in the absence of osmosis

When the capsule membrane is impermeable (i.e., $L_p = 0$), the osmosis is absent and the solvent and solute mass is conserved within each domain ($\Omega^{\pm}$). Hence, the capsule enclosed area does not change during the adhesion process. For the sake of computational efficiency, the optimal distance between the capsule and the planar substrate (d_m) is assumed to be 2.5 numbers of grid cells and equivalent to 0.625 μm. This value is relatively large compared to the values of typical biological systems which may fall in the range 10-50 nm. Similar assumptions can be seen in previous works which are on red blood cell aggregations ([33], [34]). It is believed that use of a relatively large value for d_m should not affect the main physics or trend of the adhesion behavior. Fig. 3 shows the transient of the circular capsule which is initially at a distance of d_m apart from the substrate. During the adhesion process, the capsule enclosed area is conserved with an error of less than 0.01%.

In this case, the numerical results are validated against two theoretical solutions taken from [6], [32].

For the first validation the bending rigidity is neglected (E_b = 0) so that $r_1 >> \sqrt{E_b / W_{ad}}$, where $r_1 = S_T / 2\pi$ and S_T is the total length along the membrane or simply the capsule perimeter at the equilibrium. Thus, according to the work [32], in this special case the adhesion length L_{ad} can be expressed by two characteristic lengths r_1 and r_2, where $r_2 = \sqrt{A_{eq} / \pi}$ and A_{eq} is the capsule enclosed area at the equilibrium. Hence, by means of dimensional and scaling arguments, L_{ad} is given by

$$L_{ad} \sim r_1 (1 - r_2 / r_1)^{1/3}.$$

Fig. 4 shows the comparison between this theoretical solution and the numerically calculated results obtained by changing the adhesion strength W_{ad}. For the numerically computed results the gradient of the straight line is 0.36 and it is close to the theoretical value of 0.33, which supports the validity of the present numerical approach.

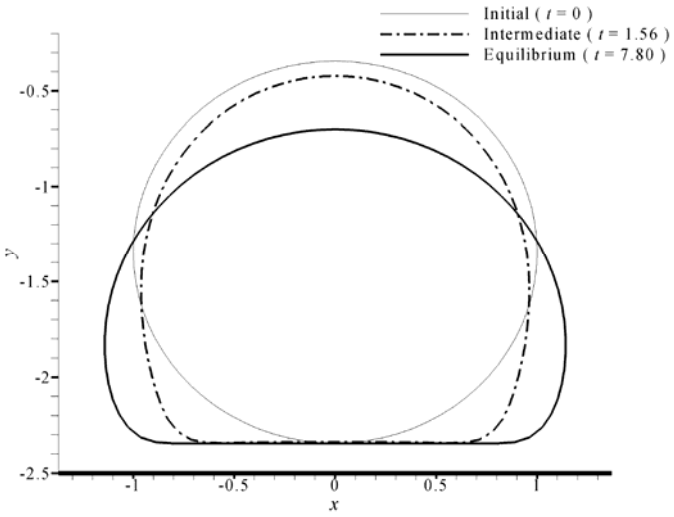

Fig. 3 Transient variation of capsule shape under adhesion onto the planar substrate: W_{ad} = 4.11 μJ/m^2, L_p = 0.

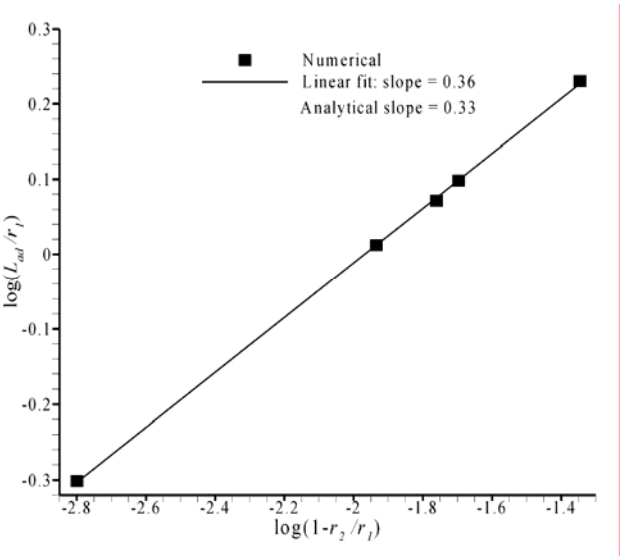

Fig. 4 Comparison between the numerical results and the theoretical solution of Contat and Misbah (1999).

Next, for the second validation the theoretical solution is derived fairly similar to the 3D elastic model reported in [6]. The assumptions are the bending is negligible and the membrane stress within the straight contact line is zero. Further, the equilibrium configuration is assumed to be a truncated circle of radius r_{eq}. Then, the law of energy conservation is applied among the potential energy of the system, elastic energy stored in the membrane and the adhesion energy of the contact line. The derivation of the model is omitted here; details are given in [6], [11] for 3D spherical capsule adhesion with planar walls. Fig. 5(a) shows

the comparison between the theoretically and numerically computed capsule shapes at the equilibrium for W_{ad} = 4.11 μJ/m^2. The agreement is reasonable for the capsule shape.

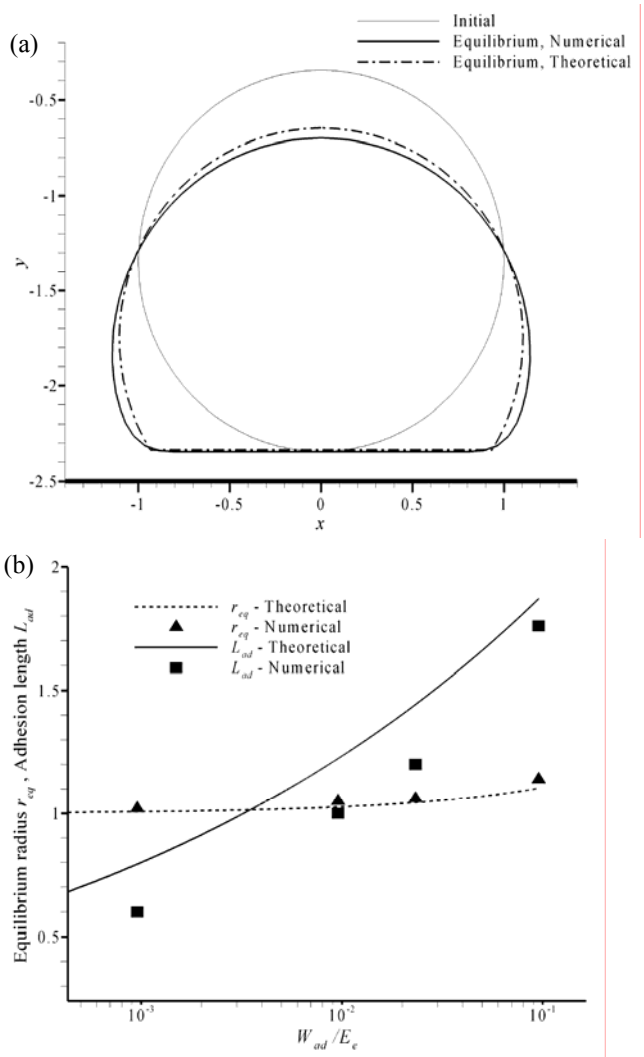

Fig. 5 Comparison between the numerical results and the results of the elastic model: (a) capsule shape at the equilibrium and (b) adhesion length and equilibrium radius of the capsule: W_{ad} = 4.11 x 10^{-2} – 4.11 μJ/m^2, L_p = 0.

The numerical and theoretical results for the adhesion length L_{ad} and the equilibrium radius r_{eq} as a function of the non-dimensional adhesion strength W_{ad}/E_e are shown in Fig. 5(b). When W_{ad} increases, the difference between the numerical and theoretical results for L_{ad} decreases while the corresponding difference for r_{eq} increases. One reason is that for stronger adhesion the equilibrium capsule geometry deviates from the circular shape and hence an average value has to be calculated for r_{eq}. Moreover, the assumption of a stress free contact line for the theoretical model may contribute to these variations between the numerical and theoretical results.

B. Adhesion in the presence of osmosis

Next, the capsule with the semi-permeable membrane (i.e., $L_p > 0$) is considered. An initial solute concentration difference is applied for the equilibrium capsule which is obtained when the osmosis is absent and W_{ad} = 4.11 μJ/m^2 (Fig. 3). Now, the solvent can pass across the membrane while the solute is not allowed to cross the membrane due to its semi-permeability. Consequently, the solute mass remains unchanged in either domain. Figs. 6(a) and (b) present the transient profiles of the membrane configuration and the solute concentration on x = 0 plane, respectively. The hydraulic conductivity of the membrane is L_p = 1x10^{-8} m^2.s/kg. The initial solute concentrations in the outer and inner domains are 27.8862 mol/m^3 and 37.8862 mol/m^3, respectively. The initial solute concentration field determines the capsule enclosed area at the equilibrium. At the equilibrium, the solvent flux across the membrane vanishes, and hence it is obtained that $f_N\delta = [c]/\ln\gamma$ from Eq. (15). By solving this non-dimensional equation fairly similar to the solution in [27], it is obtained analytically that final equilibrium enclosed area as 1.3π and the final solute concentrations at the inner and outer domains as 0.893110 and 0.893094, respectively. It is seen that the equilibrium concentration is almost the same everywhere as δ is very small ($\delta = 4.31\text{x}10^{-4}$). As observed in Fig. 6(a), the initial adhered capsule detaches gradually while the enclosed area increases from π to the equilibrium area of 1.2933π, which is very close to the analytical value of 1.3π. Fig. 6(b) shows that solute concentration jump at the membrane point nearest to the substrate which is at y = -2.5 vanishes faster than the opposite membrane point, which is the most distant point from the substrate, does. This is expected since both membrane and substrate are impermeable to solute, and hence solute distribution is restricted in the y direction. The numerically computed values of the equilibrium solute concentrations at the inner and outer domains are about 0.893626 and 0.893559, respectively, which are very close to the respective analytical values given above.

One aim of developing the model is to test the effect of some parameters on capsule adhesion with osmosis. The effect of the initial solute concentration field, hydraulic conductivity and the initial capsule geometry are tested. The influence of the initial solute concentration field on cell adhesion has been reported in previous studies. The adhesion strength is still kept at W_{ad} = 4.11 μJ/m^2 for all the cases below.

Now, the capsule detachment is tested for different initial solute concentration fields. The initial solute concentration field is changed by adjusting γ while the initial

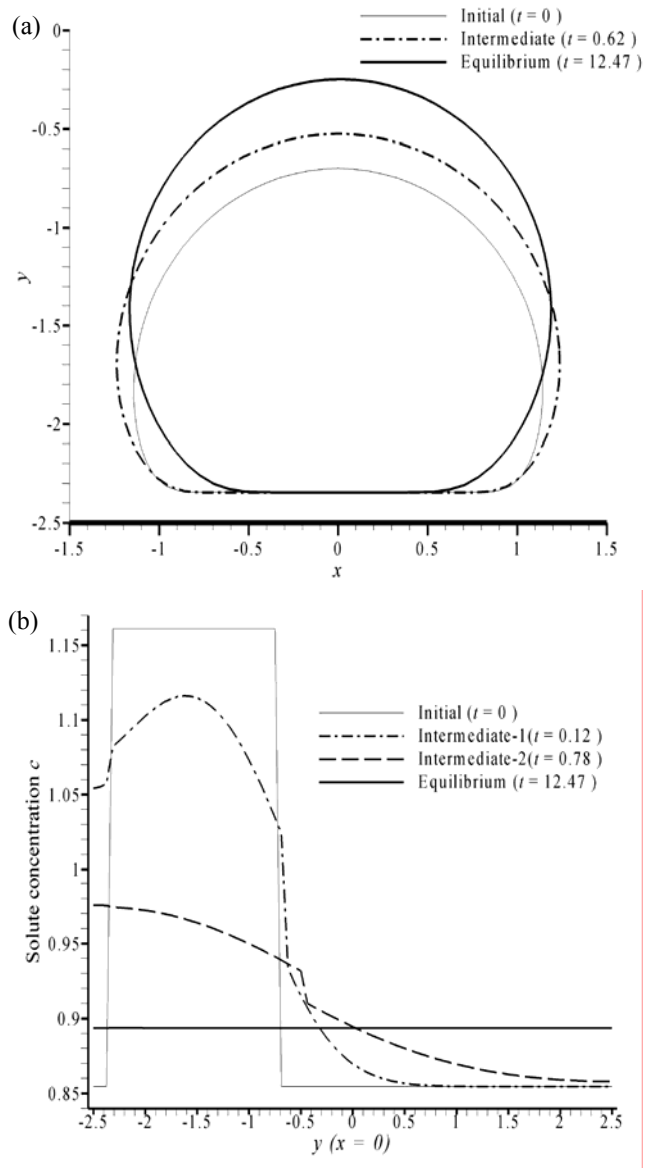

Fig. 6 Transient variation of capsule shape and solute concentration: (a) capsule shape under adhesion onto the planar substrate and (b) solute concentration filed on x = 0 plane: W_{ad} = 4.11 μJ/m^2, L_p = 1x10^{-8} m^2.s/kg, Δc_0 = 10 mol/m^3, γ = 1.3586.

concentration difference Δc_0 is kept constant at 10 mol/m^3. The initial membrane geometry is the equilibrium shape obtained with no osmosis (Fig. 3). As mentioned earlier, the final equilibrium enclosed area (A_{eq}) is a function of the initial solute concentration field (i.e., both γ and Δc_0). Therefore, the adhesion length L_{ad} and the equilibrium radius r_{eq} can be expressed as a function of $(A_{eq}\text{-}A_0)/A_0$ which is shown in Fig. 7. Here, A_0 is the initial capsule enclosed area which is equal to π . The corresponding theoretical variation is also given in the same plot. Although the numerical results of r_{eq} have good agreement with their theoretical values, the results of L_{ad} deviate from respective theoretical values for larger swelling ($(A_{eq}\text{-}A_0)/A_0$>0.6) of the capsule. Still, the variations of r_{eq} and L_{ad} qualitatively agree with previous studies which showed that adhesion length (or area for 3D capsules) decreases as the capsule inflates ([9], [11]).

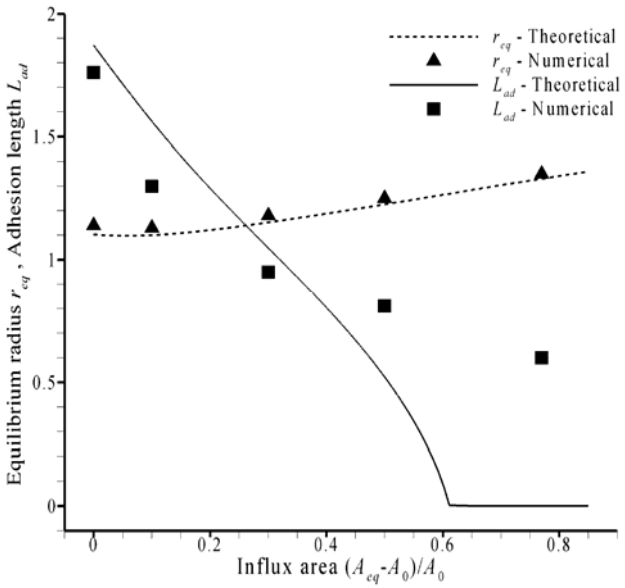

Fig. 7 Comparison between the numerical and theoretical solutions of the adhesion length and equilibrium radius of the capsule: W_{ad} = 4.11 μJ/m^2, L_p = 1x10^{-8} m^2.s/kg, Δc_0 = 10 mol/m^3, γ = 1.116-2.000.

Next, the effect of the hydraulic conductivity (L_p) on capsule adhesion in the presence of osmosis is tested. The motivation came from the published work in [35] on modeling of single plant cell compression. It has reported that the effect of the hydraulic conductivity is not significant in rapid compression of plant cells at small deformations. On the other hand, the effect of the membrane permeability properties on capsule adhesion may be important for designing drug delivery systems. The outer and inner domain solute concentrations are 27.8862 mol/m^3 and 37.8862 mol/m^3, respectively. The initial geometry is the equilibrium shape shown in Fig. 3. Two different values for L_p are chosen as 1x10^{-8} m^2.s/kg and 1x10^{-9} m^2.s/kg. Fig. 8(a) shows that L_p has no major influence on the final equilibrium shape. However, the swelling rate depends on L_p as the mass flux across the membrane is directly related to the osmotic swelling. As can be seen in Fig. 8(b), the capsule reaches the equilibrium enclosed area faster for larger L_p values.

Finally, the numerical computations are carried out for two initial geometries (Shape1 and Shape2) for the capsule. The physical parameters are L_p = 1x10^{-8} m^2.s/kg and the initial concentration field is the same as early on. As used previously, the Shape1 is the equilibrium shape obtained with no osmosis (Fig 3). The Shape2 is a circular capsule having a radius of 4 μm. Both shapes have the same enclosed area of π. As shown in Fig. 9 (a), the final equilibrium shape is identical for both initial shapes of the capsule. It can be seen from Fig 9 (b) that also swelling rate is not influenced by two initial shapes. This observation may be expected since the

initial perimeters are approximately equal in length and δ is very small; as such the solvent flux across the membrane is roughly equal for both cases as the initial concentration field is the same.

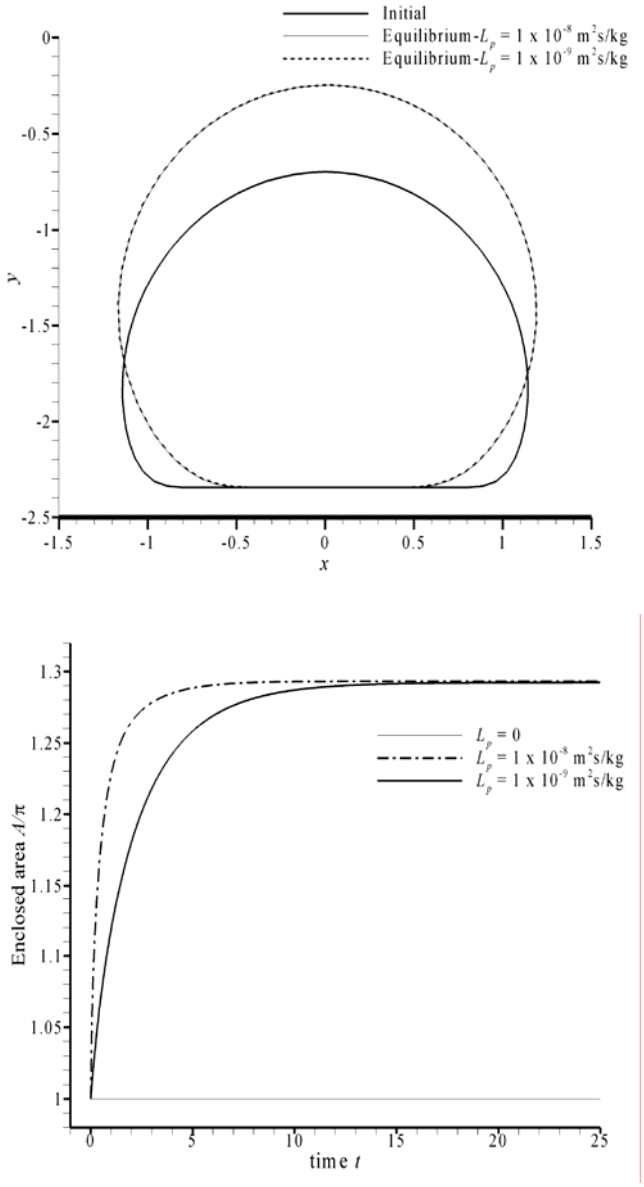

Fig. 8 Effect on the hydraulic conductivity: (a) on the final equilibrium shape of the capsule and (b) on capsule swelling: W_{ad} = 4.11 μJ/m^2, L_p = 1x10^{-9}, 1x10^{-8} m^2.s/kg, Δc_0 = 10 mol/m^3, γ = 1.3586.

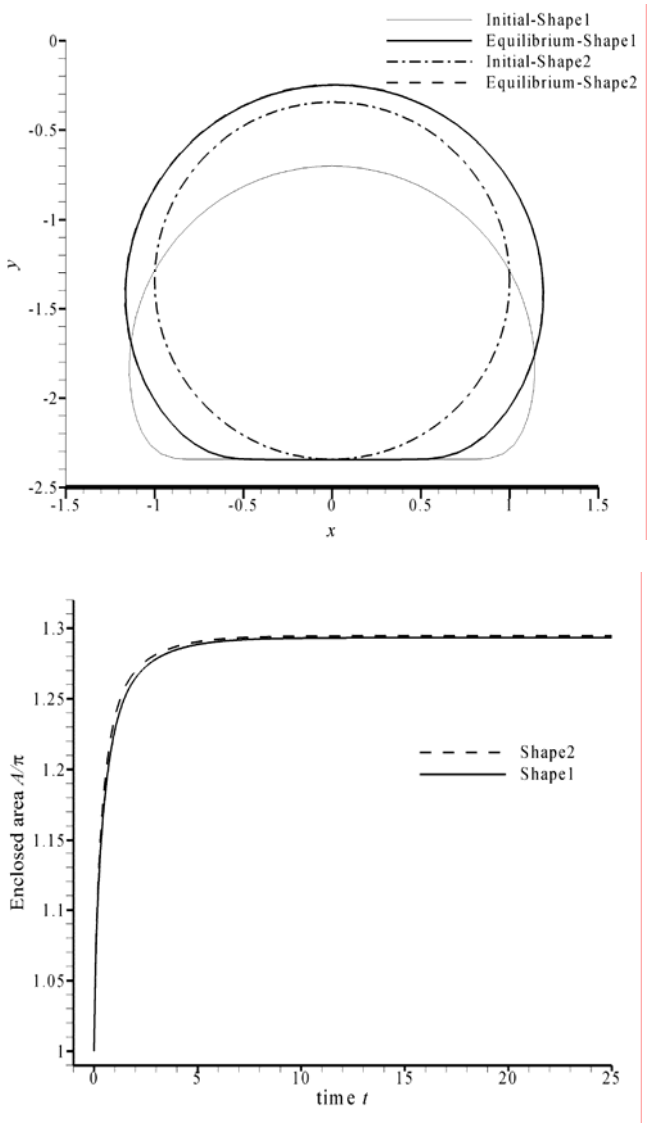

Fig. 9 Effect of the initial shape: (a) on the final equilibrium shape of the capsule and (b) on capsule swelling: W_{ad} = 4.11 μJ/m^2, L_p = 1x10^{-8} m^2.s/kg, Δc_0 = 10 mol/m^3, γ = 1.3586.

IV. CONCLUSIONS

The capsule-substrate adhesion in the presence of osmosis is simulated using the immersed interface method (IIM) under the Stokes flow condition. All the equations of motion are solved using the augmented approach reported in [29] and a new approach based on the work in [27] is built to solve the solute transport equations with the use of the Kedem-Katchalsky relation for semi-permeable membranes. The adhesion energy between the capsule and the planar substrate is represented by a potential function.

The model is applied for capsule adhesion with and without osmosis. The results are compared with two theoretical solutions and they appear reasonable. Some deviations between the results given by the numerical and the

elastic models can be attributed to the different assumptions made for the two models.

A parametric study is done to determine the effect of the initial solute concentrations, the hydraulic conductivity of the membrane and the initial capsule geometry. When the capsule adheres to the planar substrate in the binary hypotonic medium, the equilibrium adhesion length decrease as the solute concentration ratio increases since the capsule inflates much. According to the present results, the hydraulic conductivity and different initial shapes at constant enclosed area have no effect on the equilibrium shape.

The applicability of the present model is not limited to the current work. A shear flow can be easily imposed on the field by specifying a suitable velocity profile at the boundary instead of zero velocity in the present work. Also it is straightforward to use the current model to simulate adhering capsules in haptotaxis and osmophoresis which are two cell migration modes in biology ([32], [36]). These applications will be discussed in future works.

NOTATIONS

a_1, a_2, b_1, b_2 dimensions of the computational domain Ω, m

A capsule enclosed area, m^2

c solute concentration, mol/m^3

$\bar{c}$ reference solute concentration, $\bar{c} = [c_0]\ / \ln(c_0^+ / c_0^-)$, mol/m^3

$C\{\ \}$ spatial correction terms

d_m zero-force distance, m

D solute diffusivity in the fluid, m^2/s

E_b bending modulus of the membrane, J

E_e shear modulus of the membrane, N/m

$\vec{f}$ force strength, $\vec{f}(s,t) = \frac{\partial}{\partial s}\left(T_e(s,t)\vec{\tau}(s,t) + T_b(s,t)\vec{m}(s,t)\right) - \frac{\partial W}{\partial y}\hat{y}$, N/m^2

f_1, f_2 force strengths in the x and y directions, respectively, N/m^2

f_N, f_T force strengths in the normal and tangential directions, respectively, N/m^2

F_1, F_2 elastic forces in the x and y directions, respectively, N/m^3

h Cartesian grid size in both x and y directions, m

(i, j) a Cartesian grid point, dimensionless

J_v solvent volume flux across the membrane, $J_v = -L_p([p] - RT_{abs}[c])$, m^3/m^2 s or m/s

k control point on the membrane, dimensionless

L_{ad} adhesion length, m

L_p hydraulic conductivity of the membrane, m^2.s/kg

$\bar{L}_p$ reference hydraulic conductivity, m^2.s/kg

M, N numbers of x and y grid points, respectively, dimensionless

N_b numbers of control points along the membrane, dimensionless

$\vec{n}$ outward normal unit vector to the membrane, dimensionless

p fluid pressure, N/m^2

$\bar{p}$ reference pressure, $\bar{p} = \mu\bar{V} / \bar{r}$, N/m^2

Pe Peclet number, $Pe = \bar{V}\bar{r} / D$, dimensionless

Q temporal correction term

r radius of the circular capsule, m

$\bar{r}$ reference length, $\bar{r}$ = unstretched capsule radius, m

R universal gas constants, R = 8.314 J/mol.K

s length measured along the membrane, m

S_T equilibrium perimeter of the capsule, m

t time, s

$\bar{t}$ reference time, $\bar{t} = \bar{r} / \bar{V}$, s

T_e elastic tension of the membrane, $T_e(s,t) = E\left(\varepsilon^{1.5} - \varepsilon^{-1.5}\right)$, N/m

T_b shear tension of the membrane, $T_b(s,t) = \frac{\partial}{\partial s}\left[E_b(\kappa - \kappa_R)\right]$, N/m

T_{abs} absolute temperature, K

$\bar{T}$ reference membrane tension, $\bar{T} = E_e$, N/m

u, v velocity components at a Cartesian grid point in the x and y directions, respectively, m/s

U, V velocity components at a control point in the x and y directions, respectively, m/s

$\bar{V}$ reference velocity, $\bar{V} = \bar{L}_p RT\Delta c_0$, m/s

W adhesion potential, $W = W_{ad}\left[\left(\frac{d_m}{y}\right)^4 - 2\left(\frac{d_m}{y}\right)^2\right]$, J/m^2

W_{ad} adhesion strength, J/m^2

x, y Cartesian coordinate at a grid point (i, j), m

X, Y Cartesian coordinate at a control point k, m

$\hat{y}$ unit vector in the y direction, dimensionless

Greek letters

Γ, Ω membrane (interface) and computational domain, respectively

β, γ, δ $\beta = E_e / \mu\bar{V}, \gamma = c_0^- / c_0^+$, dimensionless $\delta = (E_e / \bar{r}) / RT\Delta c_0$,

δ_D two dimensional Dirac delta function, 1/m^2

μ dynamic viscosity of fluid, N.s/m^2

κ, κ_R instantaneous membrane curvature and reference curvature, respectively, 1/m

ε stretched ratio at a particular point of the membrane, dimensionless

θ the angle between the normal line to the membrane and the x axis, rad

$\vec{\tau}$ unit vector in the tangential direction to the membrane, dimensionless

Δc_0	osmotic load (i.e., initial solute concentration difference across the membrane), $\Delta c_0 = \left\| c_0^+ - c_0^- \right\|$, mol/m^3
Δt	time step width, s
$[\psi]$	jump of ψ, $[\psi(\vec{X})] = \psi(\vec{X}^+ + \zeta.\vec{n}) - \psi(\vec{X}^- - \zeta.\vec{n})$ as $\zeta \to 0^+$
Subscripts	
eq	equilibrium
i, *j*	$(i, j)^{\text{th}}$ grid point
k	k^{th} control point
n	derivative with respect to the normal direction to the membrane
o	initial ($t = 0$)
x, *y*	derivative with respect to *x* and *y*, respectively
Superscripts	
m	m^{th} time step
*	non-dimensional value
+, -	outer and inner domains, respectively

REFERENCES

[1] T. A. Springer, "Traffic signals on endothelium for lymphocyte recirculation and leukocyte emigration," Annu. Rev. Physiol., vol. 57, pp. 827-872, 1995.
[2] D. B. Khismatullin and G. A. Truskey, "A 3D numerical study of the effect of channel height on leukocyte deformation and adhesion in parallel plate flow chambers," Microvasc. Res., vol. 68, pp. 188-202, 2004.
[3] C. Dong and X. X. Lei, "Biomechanics of cell rolling: shear flow, cell-surface adhesion, and cell deformability," J. Biomech., vol. 33, pp. 35-43, 2000.
[4] V. Pappu, S. K. Doddi and P. Bagchi, "A computational study of leukocyte adhesion and its effect on flow pattern in microvessels," J. Theor. Biol., vol. 254, pp. 483-498, 2008.
[5] V. Pappu and P. Bagchi, "3D computational modeling and simulation of leukocyte rolling adhesion and deformation," Comput. Biol. Med., vol. 38, pp. 738-753, 2008.
[6] K. T. Wan and K. K. Liu, "Contact mechanics of a thin-walled capsule adhered onto a rigid planar substrate," Med. Biol. Eng. Comput., vol. 39, pp. 605-608, 2001.
[7] R. M. Servuss and W. Helfrich, "Mutual adhesion of lecithin membranes at ultralow tensions," J. Phys., vol. 50, pp. 809-827, 1989.
[8] K. D. Tachev, J. K. Angarska, K. D. Danov, and P. A. Kralchevsky, "Erythrocyte attachment to substrates: determination of membrane tension and adhesion energy," Colloid. Surface B., vol. 19, pp. 61-80, 2000.
[9] J. J. Foo, V. Chan, and K. K. Liu, "Contact deformation of liposome in the presence of osmosis," Ann. Biomed. Eng., vol. 31, pp. 1279-1286, 2003.
[10] J. J. Foo, V. Chan, and K. K. Liu, "Coupling bending and shear effects on liposome deformation," J. Biomech., vol. 39, pp. 2338-2343, 2006.
[11] K. K. Liu and K. T. Wan, "New model to characterize cell-substrate adhesion in the presence of osmosis," Med. Biol. Eng. Comput., vol. 38, pp. 690-691, 2000.
[12] K. K. Liu, V. Chan, and Z. Zhang, "Capsule-sunstrate contact deformation: determination of adhesion energy," Med. Biol. Eng. Comput., vol. 40, pp. 491-495, 2002a.
[13] K. K. Liu, H. G. Wang, K. T. Wan, T. Liu, and T. Zhang, "Characterizing capsule-substrate adhesion in presence of osmosis," Colloid. Surface B., vol. 25, pp. 293-298, 2002b.
[14] C. S. Peskin, "Numerical analysis of blood flow in the heart," J. Comput. Phys., vol. 25, pp. 220-252, 1977.
[15] N. A. N'Dri, W. Shyy, and R. Tran-Son-Tay, "Computational modeling of cell adhesion and movement using a continuum-Kinetics Approach," Biophys. J., vol. 85, pp. 2273-2286, 2003.
[16] S. Jadhav, K.Y. Chan, K. Konstantinos, and C. D. Eggleton, "Shear modulation of intercellular contact area between two deformable cells colliding under flow," J. Biomech., vol. 40, pp. 2891-2897, 2007.
[17] R. J. LeVeque and Z. Li, "The immersed interface method for elliptic equations with discontinuous coefficients and singular sources," SIAM J. Numer. Anal., vol. 31, pp. 1019-1044, 1994.
[18] Z. Li and M-C. Lai, "The immersed interface method for the Navier-Stokes equations with singular forces," J. Comput. Phys., vol. 171, pp. 822-842, 2001.
[19] M-C. Lai and H. C. Tseng, "A simple implementation of the immersed interface methods for Stokes flows with singular forces," Comput. Fluids., vol. 37, pp. 99-106, 2008.
[20] D. V. Le, B. C. Khoo, and J. Peraire, "An immersed interface method for viscous incompressible flows involving rigid and flexible boundaries," J. Comput. Phys., vol. 220, pp. 109-138, 2006.
[21] L. Lee and R. J. LeVeque, "An immersed interface method for the incompressible Navier-Stokes equations," SIAM J. Sci. Comput., vol. 25, pp. 832-856, 2003.
[22] R. J. LeVeque and Z. Li, "Immersed interface methods for Stokes flow with elastic boundaries or surface tension," SIAM J. Sci. Comput., vol. 18, pp. 709-735, 1997.
[23] Z. Li, "An overview of the immersed interface method and its applications," Taiwan. J. Math., vol. 7, pp. 1-49, 2003.
[24] M. N. Linnick and H. F. Fasel, "A high-order immersed interface method for simulating unsteady incompressible flows on irregular domains," J. Comput. Phys., vol. 204, pp. 157-192, 2005.
[25] Z. Tan, D. V. Le, Z. Li, K. M. Lim, and B. C. Khoo, "An immersed interface method for solving incompressible viscous flows with piecewise constant viscosity across a moving elastic membrane," J. Comput. Phys., vol. 227, pp. 9955-9983, 2008.
[26] S. Xu and Z. J. Wang, "An immersed interface method for simulating the interaction of a fluid with moving boundaries," J. Comput. Phys., vol. 216, pp. 454-493, 2006.
[27] A. T. Layton, "Modeling water transport across elastic boundaries using an explicit jump method," SIAM J. Sci. Comput., vol. 28, pp. 2189-2207, 2006.
[28] O. Kedem and A. Katchalsky, "Thermodynamics Analysis of the Permeability of Biological Membranes to Non-electrolytes," Biochim. Biophys. Acta, vol. 27, pp. 229–246, 1958.
[29] Z. Li, X. Wan, K. Ito, and S. R. Lubkin, "An augmented approach for the pressure boundary condition in a stokes flow," Commun. Comput. Phys., vol. 5, pp. 874-885, 2006.
[30] Z. Li and K. Ito, "The Immersed Interface Method: Numerical solutions of PDEs involving interfaces and irregular domains," USA, 2006.
[31] P. G. Jayathilake, Z.-J. Tan, B. C. Khoo, and N. E. Wijeysundera, "Deformation and osmotic swelling of an elastic membrane capsule in Stokes flows by the immersed interface method," Chem. Eng. Sci, to be published, 2009.
[32] I. Contat and C. Misbah, "Dynamics and similarity laws for adhering vesicles in haptotaxis," Phys. Rev. Lett., vol. 83, pp. 235-238, 1999.
[33] Y. Liu, L. Zhaing, X. Wang, and W. K. Liu, "Coupling of Navier-Stokes equations with protein molecular dynamics and its application to hemodynamics," Int. J. Numer. Meth. Fl., vol. 46, pp. 1237-1252, 2004.
[34] J. Zhang, P.C. Johnson, and A.S. Popel, "Red blood cell aggregation and dissociation in shear flows simulated by lattice Boltzmann method," J. Biomech., vol. 41, pp. 47-55, 2008.
[35] C. X. Wang, L. Wang, and C.R. Thomas, "Modelling the mechanical properties of single suspension-cultured tomato cells," Ann. Bot-London, vol. 93, pp. 443-453, 2004.
[36] D. Zinemanas, A. Nir, "Osmophoretic motion of deformable particles," Int. J. Multiphas. Flow, vol. 21, pp. 787-800, 1995.